GEOPHYSICAL RESEARCH LETTERS, VOL. 35, L12205, doi:10.1029/2008GL033807, 2008

High-silica deposits of an aqueous origin in western Hellas Basin, Mars

Joshua L. Bandfield[1]

Received 3 March 2008; revised 5 May 2008; accepted 20 May 2008; published 24 June 2008.

[1] Data from the Thermal Emission Spectrometer and the Thermal Emission Imaging System have been used to identify isolated high silica surfaces in western Hellas Basin. Deconvolution results indicate that the surfaces are composed of nearly 80% high silica phases (amorphous silica, phyllosilicates, or zeolites). The deposits may be derived from alcoves in the terrain immediately to the north. The high silica deposits are an additional indicator of a variety of past aqueous processes on Mars. **Citation:** Bandfield, J. L. (2008), High-silica deposits of an aqueous origin in western Hellas Basin, Mars, *Geophys. Res. Lett.*, *35*, L12205, doi:10.1029/2008GL033807.

1. Introduction

[2] An integrated view of recent spacecraft measurements has revealed a variety of surface compositions indicating that a number of aqueous and igneous processes have occurred in Mars' past. Visible through thermal infrared (TIR) wavelength spectral measurements have provided highly complementary information about the mineralogy of the Martian surface. TIR measurements from the Mars Global Surveyor (MGS) Thermal Emission Spectrometer (TES) and the Mars Odyssey Thermal Emission Imaging System (THEMIS) onboard the Mars Odyssey spacecraft have provided information about the primary surface mineralogy [e.g., *Christensen et al.*, 2001a; *Bandfield et al.*, 2000, 2004a; *Christensen et al.*, 2005; *Rogers and Christensen*, 2007]. Near-infrared measurements from the Compact Reconnaissance Imaging Spectrometer for Mars (CRISM), Mars Express Observatoire pour la Mineralogie, l'Eau, les Glaces et l'Activité (OMEGA), Imaging Spectrometer for Mars (ISM), and previous telescopic measurements have provided information about the primary igneous mineralogy from $\sim$1 and 2 μm Fe^{2+} absorptions [e.g., *Adams and McCord*, 1969; *Mustard et al.*, 1997; *Bibring et al.*, 2005].

[3] In addition, much has been learned from spectral measurements about compositions related to aqueous processes. The TES instrument has identified coarsely crystalline hematite in Meridiani Planum, Aram, Iani, and Aureum Chaos, and Valles Marineris [*Christensen et al.*, 2001b; *Glotch and Christensen*, 2005; *Glotch and Rogers*, 2007]. Laboratory studies have shown that Mars' unique Fe^{+3} absorption in visible and near infrared spectra can be attributed to nanophase hematite as well as minor amounts of crystalline iron oxides [e.g., *Morris et al.*, 1997; *Bell et al.*, 1990]. More recently, observations by OMEGA and CRISM have identified spectral features attributed to a variety of sulfate, phyllosilicate, and other hydrated compositions [*Poulet et al.*, 2005; *Gendrin et al.*, 2005; *Bibring et al.*, 2005; *Mustard et al.*, 2007]. These observations have added much towards our understanding of the igneous and climate history of Mars.

[4] Here, spectral evidence is presented for surfaces with elevated abundances of poorly crystalline to amorphous phases with high Si/O ratios (>$\sim$0.35) in western Hellas Basin. These high-silica deposits are restricted in area and their association with surface morphology is not certain. It is likely that the high-silica materials have an aqueous origin and may be similar to high-silica materials found in Meridiani Planum and Gusev Crater with Mars Exploration Rover (MER) data.

2. Data and Methods

2.1. TES/THEMIS Instruments and Data Sets

[5] THEMIS band 9 radiance images were used to construct a mosaic of the region for regional morphology (Figure 1) and daytime multispectral images were used to determine surface spectral properties. The images used for spectral analysis have average surface temperatures greater than 260 K. Daytime TES data were used to determine detailed spectral properties and surface mineralogy. More complete descriptions of the TES and THEMIS data and calibration are given by *Christensen et al.* [2001a, 2004] and *Bandfield et al.* [2004b]. Other spectral data sets, such as OMEGA with sufficient quality and CRISM, were not publicly available over the region of interest at the time of this study. THEMIS, Mars Orbiter Camera (MOC), and High Resolution Imaging Science Experiment (HiRISE) visible imagery were used for detailed morphological properties.

2.2. Analysis Methods

[6] The primary means of identifying spectrally unique localities in THEMIS data has been through inspection of decorrelation stretch (DCS) [*Gillespie et al.*, 1986] images of various THEMIS band combinations [*Bandfield et al.*, 2004a; *Bandfield*, 2006]. These data allow for a rapid assessment of spectral variability within a THEMIS image. However, it is necessary to account for atmospheric effects properly in order to retrieve quantitative spectral information. Two separate methods are used to correct for atmospheric effects in TES and THEMIS data.

[7] TES data were corrected using a method that requires ice-free atmospheric conditions and a known emissivity at 9 μm within the region (usually from dusty surfaces) for a given orbit track. Although subject to some restrictions in its use, this method removes the need for assumptions of linear approximations and a library of surface spectral endmembers

[1]Department of Earth and Space Sciences, University of Washington, Seattle, Washington, USA.

0094-8276/08/2008GL033807$05.00

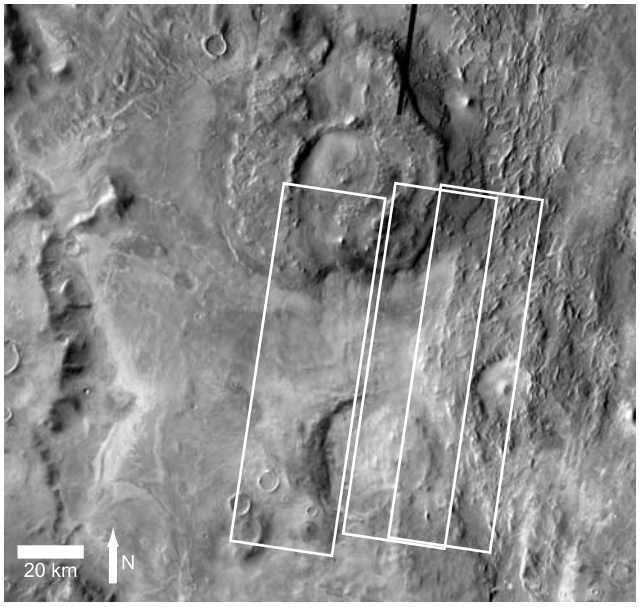

Figure 1. Daytime infrared mosaic of 45.8 to 50.0E, −40.0 to 43.0 N. White boxes indicate coverage of images shown in Figure 2. Bright areas indicate warmer surfaces covered by low albedo materials.

[*Smith et al.*, 2000] or specialized multiple emission angle observations [*Bandfield and Smith*, 2003].

[8] Minor atmospheric water vapor and CO_2 absorptions are removed using the method described by *Bandfield and Smith* [2003]. Dust aerosol loading is determined at 9 μm using nearby dusty surfaces with a known 9 μm emissivity; the 9 μm emissivity of Martian surface dust has been well constrained in a previous study [*Bandfield and Smith*, 2003]. Opacity at the region of interest is determined by assuming that the dust opacity scales with surface pressure and extending to other wavelengths using the dust opacity spectral shape of *Bandfield and Smith* [2003].

[9] THEMIS data were corrected using the methods described by *Bandfield et al.* [2004b]. Briefly, atmospheric emission and secondary scattering is calculated directly from the THEMIS data using a region of constant emissivity, but variable surface temperature. Atmospheric attenuation is then determined by defining surface emissivity for a large area within a THEMIS image from lower resolution TES data. The same atmospheric properties can be then be applied to correct each THEMIS pixel at its full spatial resolution.

[10] Linear deconvolution [e.g., *Ramsey and Christensen*, 1998] is used to determine both the distribution of spectral units within the THEMIS images as well as to determine the quantitative mineralogy from the TES data. The limited spectral information in the THEMIS data only allows for the mapping of a few spectral units and it is impossible to retrieve detailed mineralogy. Conversely, the limited spatial resolution of the TES data prevents the resolution of individual spectral units that are clearly visible in the THEMIS data. The presence of data from both TES and THEMIS within a region allows for leveraging the advantages of each data set in a manner similar to that of *Bandfield et al.* [2004a].

3. Results

[11] Decorrelation stretch THEMIS images display several distinct spectral properties (Figure 2). One spectral unit is blue in THEMIS band 6-5-4 DCS images, indicating a relatively low surface emissivity at band 6 (~10 μm). Immediately adjacent to the blue spectral unit exposures are isolated occurrences of a spectral unit that appears red in the 6-5-4 DCS images, indicating a relatively low emissivity at band 4 (~8 μm). Other regions have relatively high emissivity throughout the THEMIS spectral range and are green/yellow in the DCS images.

[12] TES and THEMIS surface spectra show significant absorption near 8–10 μm in the red spectral unit, similar to other Martian high silica surfaces (Figure 3). Because the low spatial resolution of the TES data prevents obtaining a pure measurement of the surfaces with short wavelength absorptions, contributions of mafic minerals (retrieved from deconvolution results discussed below) were removed to isolate the red unit spectral signature. This was performed in a similar manner as that of *Bandfield et al.* [2004a]. The close agreement with the higher spatial resolution THEMIS data indicates that this is a reasonable approximation of the red spectral unit surface. The blue spectral unit is spectrally similar to surface type 1 surfaces that have a basaltic mineralogy dominated by mafic minerals [e.g., *Rogers and Christensen*, 2007].

[13] The TES surface emissivity spectrum was deconvolved using a spectral endmember library similar to that of *Rogers and Christensen* [2007]. Results (Table 1) indicate high concentrations of sheet silicates/amorphous silica/

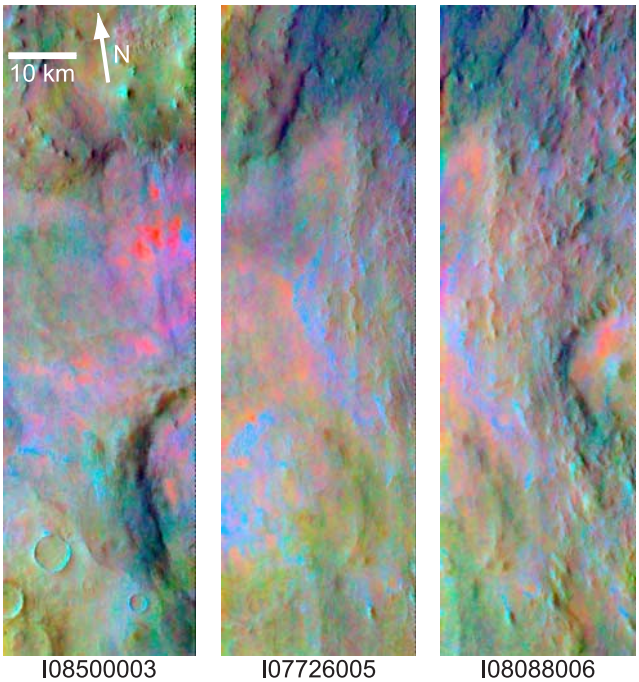

Figure 2. THEMIS band 6-5-4 DCS images showing the red, blue, and green/yellow spectral units discussed in the text.

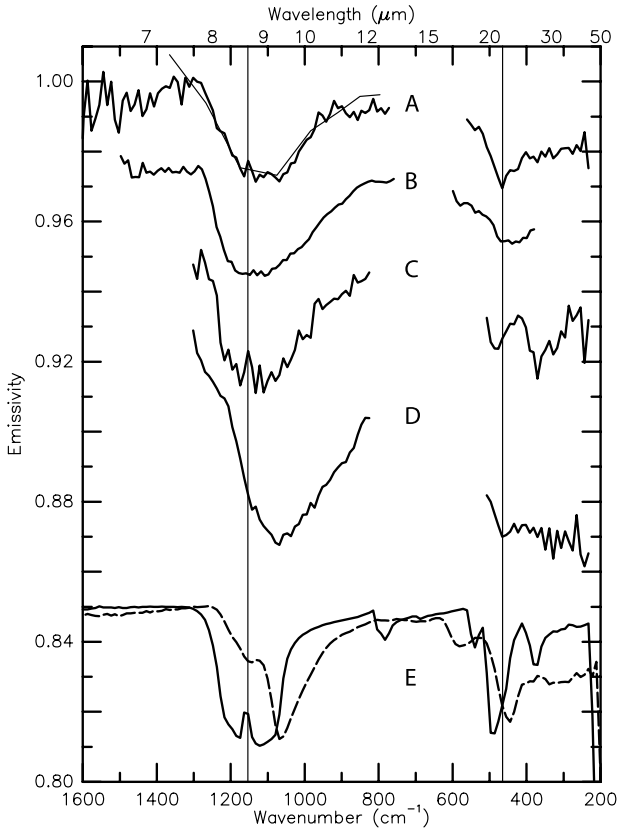

Figure 3. Martian surface and laboratory emissivity spectra: A, red spectral unit TES (from MGS orbit 4330 with mafic components removed, thick line) and THEMIS (thin line) spectra; B, amorphous silica rich Meridiani Planum outcrop spectrum [*Glotch et al.*, 2006]; C, quartz rich spectrum from near Syrtis Major [*Bandfield et al.*, 2004a]; D, amorphous silica rich surface type 2 spectrum from *Bandfield et al.* [2000]; and E, laboratory spectra of quartz (solid) and zeolite (stilbite [*Ruff*, 2004], dashed line).

zeolites/quartz (referred to here as high silica phases), sulfates, and mafic components (augite and olivine). The TES spectrum is fit well with the endmember library with a RMS error of 0.002 in emissivity and all spectral features are matched closely. As discussed above, the mafic components present in the TES surface spectrum are likely to be primarily associated with the surrounding blue spectral unit terrain with long wavelength absorptions. The derived concentrations of these components were subtracted off of the surface emissivity spectrum and the residual mineral concentrations were renormalized (Table 1). The isolated red spectral unit surface mineralogy contains 78% high silica phases and 22% sulfates. Because of the low spectral contrast, limited number of high quality spectra available, and limited areal extent, only the high silica components are considered reliable detections.

[14] THEMIS image endmembers and deconvolution were used to produce spectral unit concentration maps for THEMIS image I08500003 (Figure 4). Spectral endmembers were obtained from the THEMIS data that are correlated with red, blue, and green/yellow in the DCS images shown in Figure 2. All surfaces are fit well using these endmembers with an average RMS error of 0.001 in emissivity. The results are consistent with Figure 2, which displays an association of the red spectral unit with the more extensive blue unit.

4. Discussion

[15] The TES and THEMIS red spectral unit surface spectra display clear indications of high silica components because of the dominance of absorption at 8–10 μm with a corresponding low emissivity beyond 20 μm. A narrow absorption present in the TES data at ~22 μm is characteristic of amorphous silica, sheet silicate, zeolite, and volcanic glass phases and is distinct from that of quartz (Figure 3). Though quartz and sulfates may be present in the red spectral unit, they are not dominant phases. The deconvolution results are in agreement with the qualitative interpretation of the surface emissivity, which is also consistent with a surface dominated by high-silica and sulfate phases. Both TES and THEMIS data are consistent with the presence of isolated high silica surfaces surrounded by surfaces dominated by augite and olivine. Certain amorphous silica, sheet silicate, zeolite, and volcanic glass phases display spectral similarities that prevent their distinction in the limited TES data available [e.g., *Ruff*, 2004]. It is likely that OMEGA and CRISM near infrared data will be able to help constrain the surface mineralogy further when these data sets become available.

[16] There is some coverage of the high silica surface units with MOC and THEMIS visible wavelength imagery at 3 to 18 m/pixel spatial sampling. The mafic surrounding terrain is associated with low albedo surfaces that are commonly duneforms that are more extensive to the west (Figure 1). The high silica surfaces are relatively bright and have either a rough or lineated texture without distinct morphological boundaries. The low albedo sandy material may be responsible for scouring the high silica surfaces, keeping them free of dust or other mantling materials.

[17] The region that contains the high silica surfaces is often finely layered (examples can be found in THEMIS image V10347004, MOC image M11/00400, and HiRISE image PSP_006687_1385). Where relatively steep scarps are present, the layering shows evidence of deformation and flow, which may be indicative of the presence of ice. Most craters are heavily degraded and appear to have been partially filled and mantled. The mantling material appears to have been removed in several enclosed localities through desiccation [e.g., *Carr*, 2001]. Immediately to the north is a ~30 km diameter crater with a pedestal type morphology. Alcoves are present in the southern portion immediately to the north of the most prominent high silica deposits

Table 1. TES Surface Emissivity Deconvolution Results

Phase	Concentration (areal %)	Normalized Concentration
Sheet Silicates/Amorphous Si/Zeolites	50	75
Augite	19	–
Olivine[a]	14	–
Sulfates[a]	14	22
Quartz[a]	3	4

[a]At or below detection limits.

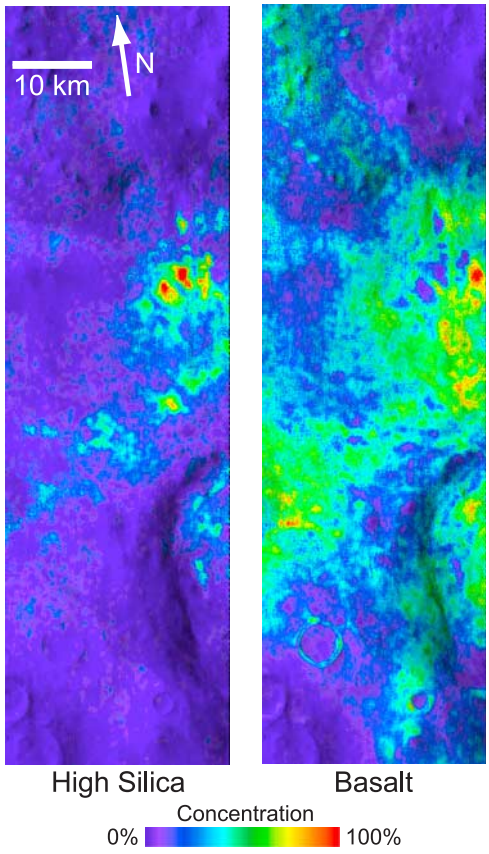

Figure 4. THEMIS spectral unit endmember concentration images derived from deconvolution of THEMIS image I08500003. The high silica concentrations are closely correlated with the red spectral unit, and the basaltic concentrations are correlated with the blue spectral unit in Figure 2.

(Figures 1 and 2). It is possible that the alcoves eroded into the hilly terrain surrounding the crater are the source of the high silica material, which may have been transported down slope.

[18] The derived mineralogy and regional morphology suggest that the high silica materials have an aqueous origin. As observed elsewhere, concentrations of high silica phases and (possibly) sulfates can be expected [e.g., *Hurowitz et al.*, 2006] as a result of aqueous alteration under Martian conditions. It is possible that the high silica phases present in this region may be concentrations of volcanic glass or phyllosilicates of a metamorphic or igneous origin (e.g. muscovite or biotite). However, the suite of minerals present is consistent with surfaces that are dominated by high-silica and sulfate phases and there is little supporting mineralogical or morphological contextual evidence for either of these scenarios.

[19] Though the layering and ice-rich terrain may have an influence on the formation of the high silica surfaces, this terrain is extensive throughout the region, whereas the high silica deposits are not. It is possible that the high silica deposits may have been formed through hydrothermal or low temperature aqueous alteration in the elevated terrain immediately to the north of the exposures. The material may have then been transported to the plains where the sand deposits scour and clean the underlying terrain, keeping the exposures uncovered.

[20] Surfaces with high silica components appear to be common on Mars (Figure 3). Quartz-rich surfaces are present near Syrtis Major [*Bandfield*, 2006]. Amorphous silica is widespread throughout Martian low albedo regions [*Bandfield et al.*, 2000a; *Ruff and Christensen*, 2007], is a major component of the outcrop rocks observed by MER in Meridiani Planum [*Glotch et al.*, 2006], and extremely high concentrations of amorphous silica (>80% SiO_2) have been identified in Gusev Crater using MER data [*Ruff et al.*, 2007]. There are distinct mineralogical and morphological differences between these deposits and it is likely that a variety of mechanisms are responsible for their origin. The Hellas high silica deposit presented here bears some resemblance to the mini-TES spectra of the outcrop material in Meridiani Planum and both surfaces are likely dominated by high-silica and sulfate phases. However, the Meridiani spectra contain significantly higher concentrations of sulfates and there are distinct differences in the shape of the $\sim$22 μm absorption. In addition, the extensive sulfate-rich materials in Meridiani Planum are not distinctive in orbital TES or THEMIS data.

[21] These five localities that have been identified with high silica components are similar in composition, yet they appear to have distinct differences in their formation mechanisms. The high silica deposits in western Hellas Basin are likely to be another indicator of a variety of past aqueous processes on Mars.

[22] **Acknowledgments.** I would like to thank Deanne Rogers for discussions about the results presented here. Tim Glotch and two anonymous reviewers provided detailed comments which improved the clarity and content of this manuscript. This work was funded in part by a grant from the Mars Data Analysis Program.

References

Adams, J. B., and T. B. McCord (1969), Mars: Interpretation of spectral reflectivity of light and dark regions, *J. Geophys. Res.*, *74*, 4851–4856.

Bandfield, J. L. (2006), Extended surface exposures of granitoid compositions in Syrtis Major, Mars, *Geophys. Res. Lett.*, *33*, L06203, doi:10.1029/2005GL025559.

Bandfield, J. L., and M. D. Smith (2003), Multiple emission angle surface-atmosphere separations of thermal emission spectrometer data, *Icarus*, *161*, 47–65.

Bandfield, J. L., V. E. Hamilton, and P. R. Christensen (2000), A global view of Martian surface compositions from MGS-TES, *Science*, *287*, 1626–1630.

Bandfield, J. L., V. E. Hamilton, P. R. Christensen, and H. Y. McSween Jr. (2004a), Identification of quartzofeldspathic materials on Mars, *J. Geophys. Res.*, *109*, E10009, doi:10.1029/2004JE002290.

Bandfield, J. L., D. Rogers, M. D. Smith, and P. R. Christensen (2004b), Atmospheric correction and surface spectral unit mapping using Thermal Emission Imaging System data, *J. Geophys. Res.*, *109*, E10008, doi:10.1029/2004JE002289.

Bell, J. F., III, T. B. McCord, and P. D. Owensby (1990), Observational evidence of crystalline iron oxides on Mars, *J. Geophys. Res.*, *95*, 14,447–14,461.

Bibring, J.-P., et al. (2005), Mars surface diversity as revealed by the OMEGA/Mars Express observations, *Science*, *307*, 1576–1581.

Carr, M. H. (2001), Mars Global Surveyor observations of Martian fretted terrain, *J. Geophys. Res.*, *106*, 23,571–23,593.

Christensen, P. R., et al. (2001a), The Mars Global Surveyor Thermal Emission Spectrometer experiment: Investigation description and surface science results, *J. Geophys. Res.*, *106*, 23,823–23,871.

Christensen, P. R., M. C. Malin, R. V. Morris, J. L. Bandfield, and M. D. Lane (2001b), Aqueous sedimentary mineralization of the Martian surface: Evidence for liquid water, *J. Geophys. Res.*, *106*, 23,873–23,885.

Christensen, P. R., et al. (2004), The Thermal Emission Imaging System (THEMIS) for the Mars 2001 Odyssey mission, *Space Sci. Rev.*, *110*, 85–130.

Christensen, P. R., et al. (2005), Evidence for magmatic evolution and diversity on Mars from infrared observations, *Nature*, *436*, 504–509.

Gendrin, A., et al. (2005), Sulfates in Martian layered terrains: The OMEGA/Mars Express View, *Science*, *307*, 1587–1591.

Gillespie, A. R., A. B. Kahle, and R. E. Walker (1986), Color enhancement of highly correlated images: I. Decorrelation and HIS contrast stretches, *Remote Sens. Environ.*, *20*, 209–235.

Glotch, T. D., and P. R. Christensen (2005), Geologic and mineralogic mapping of Aram Chaos: Evidence for a water-rich history, *J. Geophys. Res.*, *110*, E09006, doi:10.1029/2004JE002389.

Glotch, T. D., and A. D. Rogers (2007), Evidence for aqueous deposition of hematite- and sulfate-rich light-toned layered deposits in Aureum and Iani Chaos, Mars,, *J. Geophys. Res.*, *112*, E06001, doi:10.1029/2006JE002863.

Glotch, T. D., J. L. Bandfield, P. R. Christensen, W. M. Calvin, S. M. McLennan, B. C. Clark, A. D. Rogers, and S. W. Squyres (2006), Mineralogy of the light-toned outcrop at Meridiani Planum as seen by the Miniature Thermal Emission Spectrometer and implications for its formation, *J. Geophys. Res.*, *111*, E12S03, doi:10.1029/2005JE002672.

Hurowitz, J. A., S. M. McLennan, N. J. Tosca, R. E. Arvidson, J. R. Michalski, D. W. Ming, C. Schröder, and S. W. Squyres (2006), In situ and experimental evidence for acidic weathering of rocks and soils on Mars, *J. Geophys. Res.*, *111*, E02S19, doi:10.1029/2005JE002515.

Morris, R. V., D. C. Golden, and J. F. Bell III (1997), Low-temperature reflectivity spectra of red hematite and the color of Mars, *J. Geophys. Res.*, *102*, 9125–9133.

Mustard, J. F., S. Murchie, S. Erard, and J. Sunshine (1997), In situ compositions of Martian volcanics: Implications for the mantle, *J. Geophys. Res.*, *102*, 25,605–25,616.

Mustard, J. F., et al. (2007), Occurrence and stratigraphy of phyllosilicate and hydrated silicate minerals on Mars from OMEGA and CRISM, *Eos Trans. AGU*, *88*(52), Fall Meet. Suppl., Abstract P11E-03.

Poulet, F., J.-P. Bibring, J. F. Mustard, A. Gendrin, N. Mangold, Y. Langevin, R. E. Arvidson, B. Gondet, and C. Gomez (2005), Phyllosilicates on Mars and implications for early Martian climate, *Nature*, *438*, 623–627.

Ramsey, M. S., and P. R. Christensen (1998), Mineral abundance determination: Quantitative deconvolution of thermal emission spectra, *J. Geophys. Res.*, *103*, 577–596.

Rogers, A. D., and P. R. Christensen (2007), Surface mineralogy of Martian low-albedo regions from MGS-TES data: Implications for upper crustal evolution and surface alteration, *J. Geophys. Res.*, *112*, E01003, doi:10.1029/2006JE002727.

Ruff, S. W. (2004), Spectral evidence for zeolite in the dust on Mars, *Icarus*, *168*, 131–143.

Ruff, S. W., and P. R. Christensen (2007), Basaltic andesite, altered basalt, and a TES-based search for smectite clay minerals on Mars, *Geophys. Res. Lett.*, *34*, L10204, doi:10.1029/2007GL029602.

Ruff, S. W., et al. (2007), Evidence for a possible siliceous sinter deposit at home plate in Gusev Crater, *Eos Trans. AGU*, *88*(52), Fall Meet. Suppl., Abstract P23-1097.

Smith, M. D., J. L. Bandfield, and P. R. Christensen (2000), Separation of surface and atmospheric spectral features in Mars Global Surveyor Thermal Emission Spectrometer (TES) spectra, *J. Geophys. Res.*, *105*, 9589–9608.

J. L. Bandfield, Department of Earth and Space Sciences, University of Washington, Seattle, WA 98195-1310, USA. (joshband@u.washington.edu)